References

[1] Moeckel, W. E., "Approximate method for predicting form and location of detached shock waves ahead of plane or axially symmetric bodies," NACA TN 1921 (July 1949).

[2] Maslen, S. H., "Inviscid hypersonic flow past smooth bodies," AIAA J. **2**, 1055–1061 (1964).

[3] Holt, M., "Direct calculation of pressure distribution on blunt hypersonic nose shapes with sharp corners," J. Aerospace Sci. **28**, 872–876 (1961).

[4] Vaglio-Laurin, R., "On the PLK method and the supersonic blunt body problem," J. Aerospace Sci. **29**, 185–206 (1962).

[5] Johnson, R. H., "The cone-sphere in hypersonic helium above Mach number twenty," Aerospace Eng. **18**, 30–34 (February 1959).

[6] Zakkay, V. and Fields, A. K., "Pressure distributions on a two-dimensional blunt-nosed body at various angles of attack," Polytechnic Institute of Brooklyn, PIBAL Rept. 461 (October 1958).

[7] Humphrey, R. L., Little, W. J., and Seeley, L. A., "Mollier diagram for nitrogen," Arnold Engineering Development Center, AEDC TN-60-83 (May 1960).

[8] Ahtye, W. F. and Peng, T. C., "Approximations for the thermodynamic and transport properties of high temperature nitrogen with shock tube applications," NASA TN D-1303 (July 1962).

[9] Gregorek, G. M. and Korkan, K. D., "An experimental observation of the Mach- and Reynolds-number independence of cylinders in hypersonic flow," AIAA J. **1**, 210–211 (1963).

[10] Hamaker, F. M., "Numerical solution of the flow of a perfect gas over a circular cylinder at infinite Mach number," NASA Memo. 2-25-59A (March 1959).

[11] Fuller, F. B., "Numerical solutions for supersonic flow of an ideal gas around blunt two-dimensional bodies," NASA TN D-791 (July 1961).

[12] Penland, J. A., "Aerodynamic characteristics of a circular cylinder at Mach number 6.86 and angles of attack up to 90°," NACA TN 3861 (1957).

[13] Greenberg, R. A., "A correlation of nose-bluntness-induced pressures on cylindrical and conical afterbodies at hypersonic speeds," J. Aerospace Sci. **29**, 359 (1962).

[14] Chernyi, G. G., *Introduction to Hypersonic Flow* (Academic Press, New York, 1961).

[15] Cheng, H. K., Hall, J. G., Golian, T. C., and Hertzberg, A., "Boundary-layer displacement and leading-edge bluntness effects in high-temperature hypersonic flow," J. Aerospace Sci. **28**, 353–381 (1961).

[16] Cheng, H. K., "Hypersonic flow with combined leading-edge bluntness and boundary-layer displacement effect," Cornell Aeronautical Lab. Rept. AF-1285-A-4 (August 1960).

SEPTEMBER 1964 AIAA JOURNAL VOL. 2, NO. 9

Recent Studies of the Laminar Base-Flow Region

ERIC BAUM,* HARTLEY H. KING,† AND M. RICHARD DENISON‡

Electro-Optical Systems, Inc., Pasadena, Calif.

Some recent theoretical studies of the fluid dynamics and energy transport in the laminar base-flow region are presented. Improvements to Chapman's separated flow analysis include the effect of finite initial profiles at the separation point, the effects of mass injection from the body surface or base, and the influence of base heat transfer. Some of the more important conclusions are that 1) the Crocco integral relation for the enthalpy and atom distributions in the separated shear layer is not valid for most hypersonic bodies because the base-flow region is far too short for the profiles to have become similar; 2) the distortion of initial profiles due to a sharp turn at the separation point results in a shorter and cooler base flow, as compared to using undistorted initial profiles; 3) base heat transfer appears to have only a slight effect on base-flow properties; and 4) both base gas injection and similar blowing from the body wall result in a cooler and longer base-flow region, base injection being the more effective in cooling the wake for equal mass injection rates.

Nomenclature

B = blowing parameter
DSL = dividing streamline
E = auxiliary enthalpy function, Eq. (12)
ESL = inviscid flow streamline outside viscous layer, Fig. 3
F = shear function, Eq. (6)
f = Blasius function
H = total enthalpy, $h + u^2/2$
k = 0 for two-dimensional flow, 1 for axisymmetric flow
M = Mach number
$\dot{M}$ = injection mass flow rate (per unit depth, two-dimensional, total, three-dimensional)
Re = Reynolds number
r_0 = radius of viscous layer
S = reduced streamwise distance, Eq. (4)
SSL = stagnating streamline
u = streamwise velocity
v = transverse velocity
W = auxiliary enthalpy function, Eq. (12)
x = streamwise distance
Y = transformed normal distance, Eq. (7)
y = transverse distance
z = distance along centerline from base
α = cone half angle
β = wake angle
μ = viscosity
ρ = density
τ = shear stress
ψ = stream function

Subscripts

b = base wall
c = recirculating core

Presented as Preprint 64-5 at the AIAA Aerospace Sciences Meeting, Pasadena, Calif., January 20–22, 1964. This research was sponsored by the Advanced Research Projects Agency, Department of Defense under ARPA Order 203-A1-63. The authors are indebted to Lester Lees of the California Institute of Technology, Martin H. Bloom of the Polytechnic Institute of Brooklyn, and Andrew Hammitt and Leslie Hromas of Space Technology Laboratories for many valuable discussions.

* Senior Scientist. Member AIAA.
† Senior Engineer. Member AIAA.
‡ Manager, Gas Dynamics Department. Member AIAA.

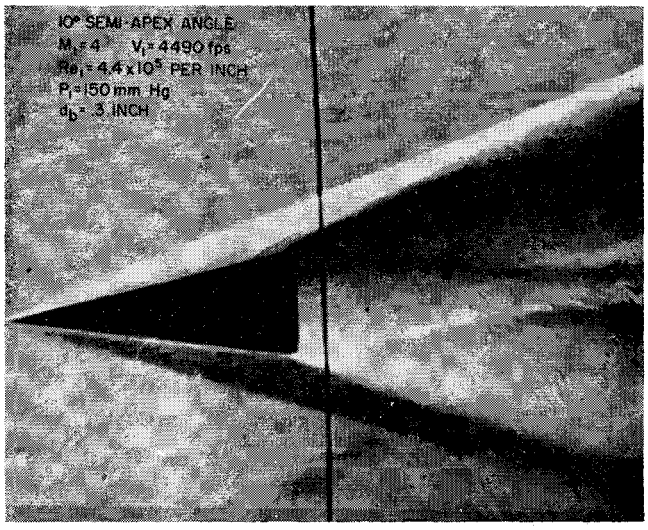

Fig. 1 Cone in free flight.

D = dividing streamline
e = outer edge of viscous layer
i = injected gas
s = stagnating streamline at recompression
w = body wall
1 = freestream
2 = inviscid flow outside body wall
3 = inviscid flow outside shear layer
4 = inviscid flow behind trailing shock

Introduction

THE investigation of the laminar base-flow region of hypersonic bodies was begun years ago, primarily with the aim of predicting base pressure. In recent years, there has been a resurgence of interest in this problem because of its importance in the prediction of downstream wake properties. For slender bodies in particular, where the inviscid flow is relatively cool, downstream wake calculations are strongly dependent on the initial conditions at the wake neck. The primary objective of the series of investigations which will be described here was to develop an improved theoretical description of the laminar base-flow region so that the properties within the base-flow region and the initial conditions for the downstream wake could be more accurately predicted.

A schlieren photograph§ and a corresponding schematic diagram of the laminar hypersonic base flow are shown in Figs. 1 and 2. The hypersonic outside flow is separated from the relatively low velocity core of the base-flow region by a separated shear layer, and this shear layer has an initial thickness and structure that are due to the body boundary layer. A dividing streamline (*DSL*) originates at the separation point and is the inner boundary of the flow originating upstream (from the body boundary layer). A stagnating streamline (*SSL*) separates the flow that continues downstream through the neck from that which turns back and recirculates. In the absence of base gas injection, the *DSL* and *SSL* coincide; when there is base gas injection, the rate of gas flow between the *DSL* and *SSL* corresponds to the injection rate.

The analysis of the base flow is considerably simplified when the model of Chapman[1-4] is employed, because this permits subregions of the base flow to be solved independently and then coupled together. The base-flow geometry is determined by assuming that the shear layer is thin and the recompression region is small in extent, so that the total pressure on the stagnating streamline is recovered at the rear stagnation point and is equal to the static pressure behind the trailing shock (determined by the inviscid flow). Using this model, Chapman found a similar solution to the velocity profiles in the separated shear layer, and his solution is valid when the separated shear layer has no initial thickness, or if it is sufficiently long that the effect of the initial velocity distribution is negligible.

Two of the present authors[5] have more recently performed a nonsimilar separated shear layer calculation by means of a finite difference method within the framework of Chapman's model, in which the initial profile was assumed to be the Blasius velocity distribution. By making some assumptions about the enthalpy profiles, the analysis could be applied to the determination of the base-flow properties of cones and wedges, and it was found that the length of the shear layer from the body to the neck was far too short to reach the asymptotic velocity distribution of Chapman.

These results motivate the extension of the analysis to include profiles of total enthalpy and atomic species concentration.[6] In order to do this, it is assumed that $Le = Pr = 1$. Then, in the spirit of the Chapman model, it is assumed that the separated shear layer is a thin mixing zone between the outer flow and the essentially stagnant inner recirculating core. The core region itself is assumed to have a bulk or average total enthalpy H_c, which is constant but initially unknown. This unknown parameter is later determined as part of the solution to the problem by requiring that over-all energy and mass balances for the base-flow region be satisfied.

The present paper contains a summary of several recent investigations[6-11] based on this model. These studies, previously unreported in the open literature, include:

1) Calculations of the total enthalpy and atom species concentration profiles, assuming initial conditions given by the Blasius solution for velocity, and Crocco integral relation for enthalpy and atom composition.

2) Calculations of the effect on the subsequent separated shear-layer profiles of a sharp turn at the separation point. Instead of stretching the coordinates, but retaining the Blasius distribution after expansion (as in item 1), the boundary-layer gas is assumed to be expanded isentropically along streamlines. The initial conditions then correspond to a distorted Blasius and Crocco distribution, the degree of distortion determined by the turning angle at the separation point.

3) Calculations of the recirculating region flow field by means of potential flow matched to the inside of the shear layer and estimation of base heat transfer and its effect on the base-flow configuration.

4) Calculations of the effects of similar blowing on the body surface and of gas injection from the body base on the separated shear-layer profiles.

From the point of view of the numerical calculations, these investigations represent variations in the initial conditions for the separated shear layer or in the over-all balance relations. The method of calculation will be described for the general case in which all of these possibilities are considered. Then the specific investigations enumerated previously will be

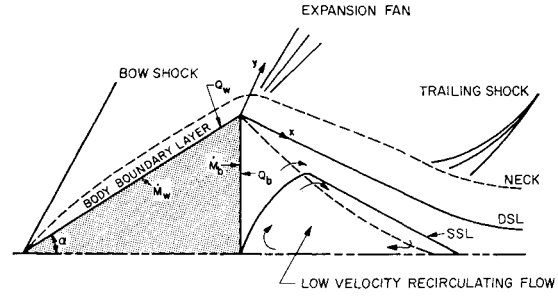

Fig. 2 Base-flow region.

§ The authors express their appreciation to Jerome Eckerman of AVCO Research and Advanced Development for permission to publish this photograph.

summarized. More detailed results, including tabular listings of profiles and integrals appearing in the balance relations, can be found in the cited references.

Method of Calculation

Conservation Equations

The equations describing the flow in the separated shear layer are obtained by applying the usual hypersonic transformations to the boundary-layer equations.[5] The assumptions made are that $\rho\mu = \text{const}$, $Le = Pr = 1$, and $dP/dx = 0$. For numerical work the Crocco coordinate system is used so that the final form of the shear-layer equations becomes

Momentum

$$u^*(\partial F_*/\partial S^*) = F_*{}^2(\partial^2 F_*/\partial u_*{}^2) \tag{1}$$

Energy

$$u^*(\partial H/\partial S^*) = F_*{}^2(\partial^2 H/\partial u_*{}^2) \tag{2}$$

For a Lewis number of unity, the extension of the analysis to include atom species concentrations is straightforward[6] and will not be included here for lack of space.

The dependent variables are the shear function $F_*(S^*,u^*)$ and the total enthalpy $H(S^*,u^*)$. In Eqs. (1) and (2), the following definitions were employed:

$$u^* = u/u_e \tag{3}$$

$$S^* = S/S_w \quad \text{where} \quad S = \int C\rho_e u_e \mu_e r_0{}^{2k}\, dx \tag{4}$$

$$C = \rho\mu/\rho_e\mu_e \text{ (Chapman-Rubesin constant)} \tag{5}$$

$$F_* = FS_w{}^{1/2} \quad \text{where} \quad F = \partial u^*/\partial Y \tag{6}$$

$$Y = u_e r_0{}^k \int \rho dy \tag{7}$$

In Eq. (4), S_w is measured along the body from the nose to the separation point, and S is measured downstream from the separation point ($x = 0$). The inner edge boundary conditions for Eqs. (1) and (2) are as follows:

$$F^*(S^*,0) = 0 \tag{8}$$

$$H(S^*,0) = H_c \text{ (unknown core enthalpy)} \tag{9}$$

The outer-edge boundary conditions are

$$F^*(S^*,1) = 0 \tag{10}$$

$$H(S^*,1) = H_e \tag{11}$$

The initial conditions are determined by the body boundary-layer shear and total enthalpy profiles. In this paper we assume that the body boundary-layer shear profile is given by the Blasius solution, with the Crocco integral relation for the total enthalpy. If the effect of the sharp turn at separation is neglected, then these profiles will also be the initial conditions for the separated shear layer. However, we shall also discuss cases in which the boundary-layer profiles distort at separation according to an isentropic expansion to the base pressure along streamlines. In this case, the distorted profiles become the shear-layer initial conditions.

Because the unknown core enthalpy H_c is a boundary condition, the numerical solution is somewhat unconventional. The object of the method employed is to arrange the equations and boundary conditions so that the numerical solution can be carried out without knowing the quantity H_c. This can be done, since Eq. (1) is uncoupled from (2), and Eq. (2) is linear in H. Therefore H can be replaced by a linear combination of new functions of S^*, u^* with the constant H_c appearing as a multiplier. Thus new functions $W(S^*,u^*)$ and $E(S^*,u^*)$ are introduced such that

$$H - H_e = (H_w - H_e)W + (H_c - H_e)E \tag{12}$$

Then H will be properly calculated if both W and E satisfy Eq. (2) (replacing H), and if the following boundary and initial conditions are satisfied:

$$W(S^*,0) = W(S^*,1) = E(S^*,1) = 0 \tag{13}$$

$$E(S^*,0) = 1 \tag{14}$$

$$W(0,u^*) = [(H - H_e)/(H_w - H_e)]_{S^*=0} \tag{15}$$

$$E(0,u^*) = 0 \tag{16}$$

In the special case in which the initial conditions are given by the Crocco integral, the function E reduces to the quantity $(1 - u^* - W)$, and the initial condition is then $W(0,u^*) = 1 - u^*$.

Starting Solution

A singularity at the separation point caused by the discontinuity in boundary conditions at the inner edge of the shear layer causes difficulty in starting the numerical solution. Although the singularity is mathematical rather than physical because the basic equations are not valid in this local region, it is desirable to obtain a self-consistent starting solution. This difficulty was overcome by obtaining a power series solution valid near the discontinuity (i.e., small S^* and u^*). For example, when the initial profile is a Blasius profile with similar blowing, the velocity profile near the wall is characterized by a linear relation between shear function and velocity. A sublayer is then defined, with boundary conditions

$$u^* = 0 \qquad F^* = 0$$

$$u^* \to \infty \qquad F^* \to F^*{}_w(1 + Bu^*)$$

The series solution of the sublayer is then chosen to be of the form

$$F^* = F^*{}_w\{F^{(0)}(\xi) + F^{(1)}(\xi)B(3S^*F_w{}^{*2})^{1/3} + \ldots\} \tag{17}$$

where

$$\xi = u^*/(3S^*\, F_w{}^{*2})^{1/3}$$

$$B = -[f(0)/f''(0)] = \dot{m}_w u_e/\tau_w$$

The choice of ξ as an independent variable was suggested by the solution of Goldstein,[12] who found for the wake of a flat plate in incompressible flow that the velocity grows as $x^{1/3}$. The resulting differential equations are presented and solved in a note in the AIAA Journal.[13] These "transition" profiles are then patched onto the remainder of the initial profiles at a small value of u^* and a very small value of the streamwise distance parameter S^* (say, at about $S^* = 10^{-8}$). The starting difficulty is thereby overcome, and the calculations proceed by an implicit finite difference method.[5]

Over-All Energy Balance

To derive an expression for the unknown core enthalpy H_c, the requirement that an over-all energy balance for the base flow region be satisfied is imposed. The system boundaries for the case of no base mass injection are shown in Fig. 3, and the extension to the case of base bleed presents no difficulty. The system is bounded on the upstream end by the plane of the base of the body, at the downstream end by the wake neck, and at the sides by a streamtube (ESL) in the inviscid flow just outside the shear layer. Mass (and the energy associated with it) enters the system through the shear layer leaving the body and leaves through the shear layer passing downstream through the neck of the wake. If there is injection of gas into the recirculation region through the base wall, this is an additional source of mass and energy. Energy can

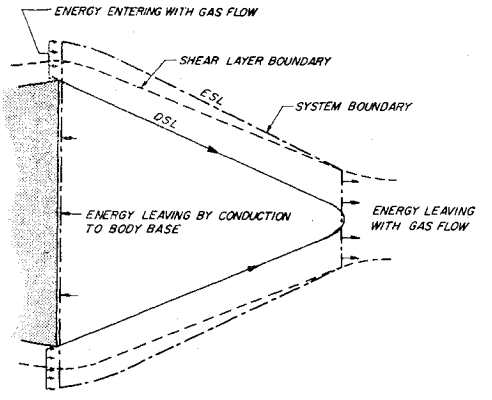

Fig. 3 System boundary for energy balance.

also leave the system by heat transfer to the base of the body. The energy balance is therefore written

$$\left[-\int_{DSL}^{ESL}(H_e - H)\rho u(2\pi r_0)^k dy\right]_{\text{body}} + [-(H_e - H_i)\dot{M}] =$$

energy entering from body boundary layer¶ — energy entering due to base bleed

$$\left[-\int_{SSL}^{ESL}(H_e - H)\rho u(2\pi r_0)^k dy\right]_{\text{neck}} + Q_b$$

energy leaving through neck — energy leaving by heat conduction to base and radiation

(18)

By making a suitable change of coordinate system to that used in the numerical calculations, this equation can be reduced to the form

$$H_e = H_e - \frac{(H_e - H_w)(K - J) + [Q_b/(2\pi)^k - (H_e - H_i)\psi_s]/S_w^{1/2}}{L} \quad (19)$$

where

$$J(S^*_s) \equiv \left[\int_{u_s^*}^{1} \frac{u_* W}{F_*}\, du_*\right]_{\text{neck}}$$

$$K \equiv \left[\int_{0}^{1} \frac{u_*(1 - u_*)}{F_*}\, du_*\right]_{\text{body}}$$

$$L(S^*_s) \equiv \left[\int_{u_s^*}^{1} \frac{u_* E}{F_*}\, du_*\right]_{\text{neck}}$$

The stream function ψ_s corresponding to the stagnating streamline is found from an over-all mass balance, and is related to the base bleed rate $\dot{M}_w$ by

$$\psi_s \equiv \int_{DSL}^{SSL} \rho u\, r_0^k dy = S_w^{1/2}\int_{u_s^*}^{u_s^*} \frac{u_* du_*}{F_*} = -\frac{\dot{M}_w}{(2\pi)^k} \quad (20)$$

It should be noted that an analogous development may be employed for the treatment of atomic species profiles and the atom species mass fractions in the recirculating core.[6]

Matching with the Inviscid Flow

To carry out the matching of the shear layer and inviscid regions, the body shape, freestream conditions, body surface enthalpy H_w, and base enthalpy H_b must be specified. (H_b need not be specified if the base heat-transfer rate is negligible, which we will later see is almost always a good assumption and will be used in this report unless otherwise noted.)

¶ An integral energy balance applied to the body shows that the first integral of Eq. (18) is equal to Q_w, the total heat transferred to the upstream body surface.

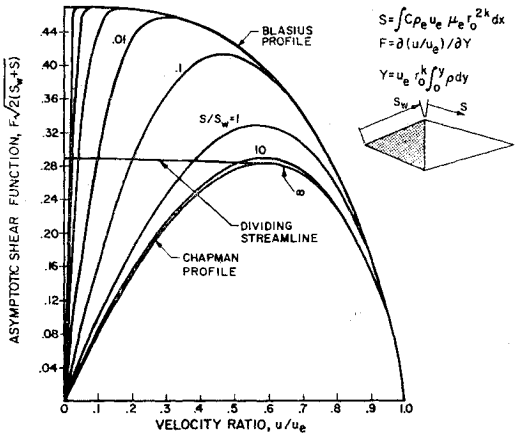

Fig. 4 Shear function profiles.

For simplicity, in the present paper attention is restricted to assumed perfect gas conditions for pointed cone bodies. A simplified inviscid flow model is employed, consisting of a Taylor-Maccoll flow on the body, a Prandtl-Meyer expansion to the base pressure, a constant pressure shear layer, and an isentropic recompression at the neck. The curvature of a constant pressure line in axisymmetric flow is neglected.

The static pressure P_4 behind the trailing shock is defined by the inviscid calculation for any trial wake angle β. The stagnating streamline total pressure may be calculated from the static pressure P_3 plus the $\rho u_s^2/2$ obtained from the shear-layer solution at S_s^*. With the present simplified model, S_s^* depends on the trial wake angle β and other flow parameters as follows:

$$S_s^* = \frac{C_3\rho_3 u_3 \mu_3 \sin\alpha}{C_2\rho_2 u_2 \mu_2 \sin\beta}$$

Matching occurs at the value of β for which Chapman's recompression condition is satisfied. A separate computer program was written to carry out this matching procedure, and solutions for a wide range of conditions are presented in Ref. 11. Some typical data (assuming $C_3/C_2 = 1$ and $\mu \propto T^{0.76}$) are given in this paper to illustrate the type of results obtained.

Results—No Mass Injection

Equations (1) and (2) have been solved for a variety of initial profiles, but it is not possible to include all of these results here. Figure 4 shows the behavior of the shear stress

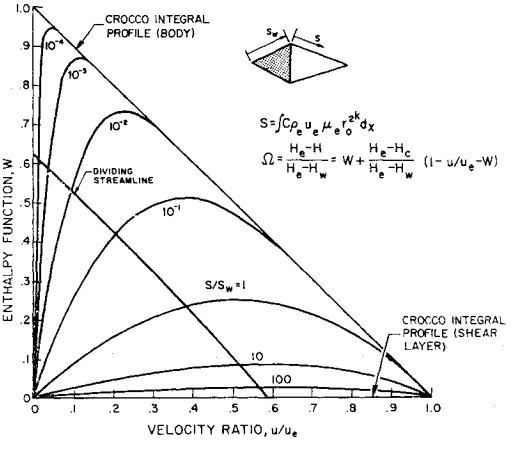

Fig. 5 Profiles of enthalpy function W.

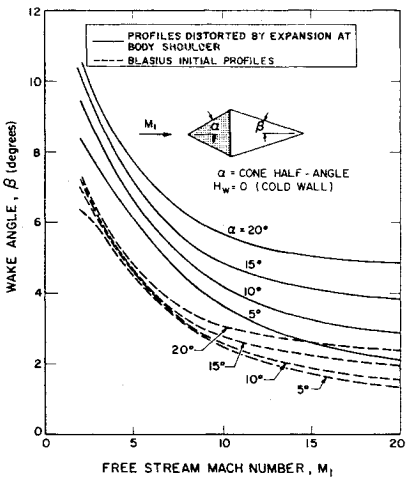

Fig. 6 Effect of initial profile distortion on the wake angle.

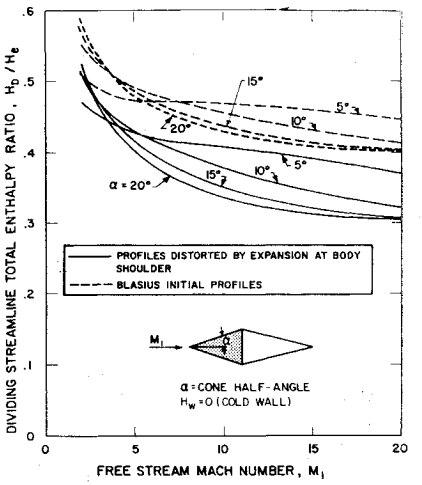

Fig. 7 Effect of initial profile distortion on the neck centerline enthalpy.

function $F(S^*,u^*)$ for the case where the initial velocity is a Blasius profile. By plotting the results with ordinate $F[2(S + S_w)]^{1/2}$, the transition of the profile from the initial Blasius values to the asymptotic Chapman values as $S^* \to \infty$ can be seen.

Figure 5 gives the $W(S^*,u^*)$ profile corresponding to initial conditions using the Blasius velocity profiles with the Crocco integral relation for total enthalpy. Note that $W \to 0$ slowly as $S^* \to \infty$, which, from Eq. (12), means that the Crocco integral relation will be valid for the shear layer only if it is extremely long. The results show that, after the shear layer is matched to the outer inviscid flow, its length S_s^* is usually less than unity. Therefore, all actual profiles in the shear layer $0 < S^* < S_s^*$ are far from fully developed, and the Crocco integral relation is not valid anywhere in the separated region.

Profile Distortion at Separation

The dashed curves of Fig. 6 give for various freestream Mach numbers the predicted wake angle for various cold-wall cones ($H_w = 0$). If it is assumed that the initial profiles distort due to the expansion at the body shoulder (such that the flow is isentropic along streamlines), then new initial shear-layer profiles occur.** The severity of the expansion is a function of the Mach number ratio M_2/M_3, which in turn depends on the trial wake angle β. Thus the matching calculation is somewhat more complicated than that described previously.

The importance of this effect is indicated in Fig. 6. When the shoulder expansion is included, the predicted wake angles are considerably larger than those previously obtained. Unfortunately, with $H_w \neq 0$, a gap in the initial velocity profile occurs at the inner edge due to the expansion ratio, and these cases have not as yet been analyzed. Thus for cases where $H_w \neq 0$, conclusions regarding the effects of the shoulder profile distortion must remain tentative.

The centerline total enthalpy H_D at the neck is shown in Fig. 7, and again the effect of including the shoulder expansion in the analysis is evident. For example, for a 10° cone at $M_1 = 20$, the predicted H_D/H_e is about 0.42 without the body shoulder expansion effect, but only 0.31 when this effect is included. This could make a considerable difference in downstream wake calculations.

The initial profile distortion due to expansion at the shoulder produces a large effect on the base flow primarily because the initial profiles become much more "full" than the Blasius profile. This causes the velocity and the corresponding total pressure along the dividing streamline to build up with distance at a much greater rate. Figure 8 shows this velocity build-up for various expansion Mach number ratios M_2/M_3. We note parenthetically that final matching usually yields about 0.6 for this ratio, and that the rate of enthalpy build-up along the stagnating streamline is relatively unaffected by the profile distortion. Thus, including the initial profile distortion causes Chapman's recompression condition to be satisfied at a smaller S_s^* value, and this produces a larger wake angle. The whole temperature or static enthalpy level of the base flow is thereby lowered, because not as much high velocity gas will enter the shear layer and be slowed relative to the body.

Base Heat Transfer

Another feature that may affect the over-all base flow solution is base heat transfer. The use of an over-all energy balance to determine the core enthalpy was presented previously, and it is obvious that the base heat transfer will alter this balance. This effect has been studied by extending the Chapman model to include some details of the recirculating flow. Thus, to calculate the shear layer, the assumption of zero velocity in the recirculating core is retained, and the Chapman-type matching with the inviscid flow is carried out. In order to estimate base heating effects, it is then assumed that the flow in the core is a low-speed potential flow outside a stagnation-point-type boundary layer existing on the base wall. This base-wall layer provides a thermal resistance be-

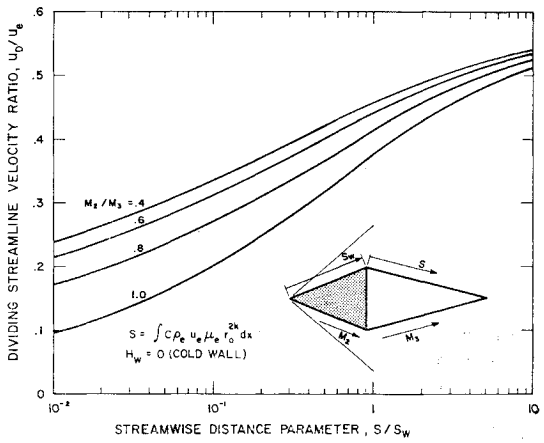

Fig. 8 Effect of initial profile distortion on the dividing streamline velocity buildup.

** The initial enthalpy profile for the shear layer is no longer given by the Crocco integral, although the Crocco integral applies before the expansion.

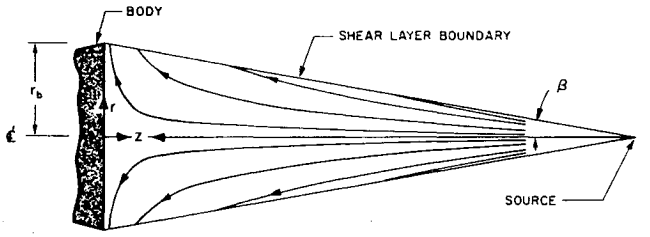

Fig. 9 Recirculating core flow field.

tween the base wall at enthalpy H_b and the bulk core region at enthalpy H_c. The induction of fluid along the inner edge of a separated shear layer (i.e., the normal velocity component) provides a driving force for the recirculating flow, with mass conservation being maintained by introducing a "source" at the recompression end of the shear layer (Fig. 9). The problem to be solved is then as follows:

$$\frac{\partial^2\psi}{\partial z^2} + \frac{\partial^2\psi}{\partial r^2} - \frac{k}{r}\frac{\partial\psi}{\partial r} = 0$$

with boundary conditions

$$\psi = 0 \text{ on the base wall}$$

$$\psi = 0 \text{ on the centerline}$$

$$\psi = \psi_c \text{ on the shear layer}$$

In the preceding, $\psi_c(x)$ is given by the shear-layer solution. The solution of this recirculating flow region then provides outer boundary conditions for the base-wall boundary-layer calculation, and hence an estimate of the base heat transfer. The shear-layer/inviscid-flow matching is then repeated, until all features of the base-flow match, with the exception of the tangential velocity along the inner edge of the shear layer. This last quantity cannot be made to match properly, since only the normal velocity component can be specified in the recirculating potential flow region.

If the recirculating flow model just outlined is used, and the boundary-layer calculations of Cohen and Reshotko[14] are employed, the base heat-transfer term for cones may be written approximately in the form

$$Q_b \propto (H_c - H_b)/(Re_1)^{1/4} \tag{21}$$

The proportionality constant in (21) is also a weak function of other quantities involved in the matching, but this shows the major parameters affecting Q_b. If this equation is now coupled into the matching process through the energy balance Eq. (19), the whole base flow solution will be affected. The importance of the base heating term depends on relative magnitudes of $Q_b{}^*$ and $(K\text{-}J)$, where

$$Q_b{}^* = \frac{Q_b}{(2\pi)^k(H_e - H_w)} = K\frac{Q_b}{Q_w} \tag{22}$$

and Q_w is the total heat transferred to the upstream body surface. The latter equality follows from an energy balance applied to the body alone.

Figure 10 gives the predicted base heat-transfer rate for some typical conditions. For these conditions, the total base heat transfer is only of the order of 0.002 to 0.006 of the body total heat transfer for Reynolds numbers of interest. From the shear-layer solution, it is found for these conditions that $(K\text{-}J)/K$ is of order 0.1, which is large compared to the range 0.002 to 0.006. Thus the influence of base heat transfer on the base flow is probably negligible according to this model, especially at high Mach numbers.

Because of the approximate nature of the recirculating flow theory and the calculation of base heat transfer, it is of interest to determine the sensitivity of the core enthalpy calculation to the base heat-transfer rate. Various values of Q_b can be assumed arbitrarily, and the base-flow matching can be carried out as before (say, using the shear-layer data

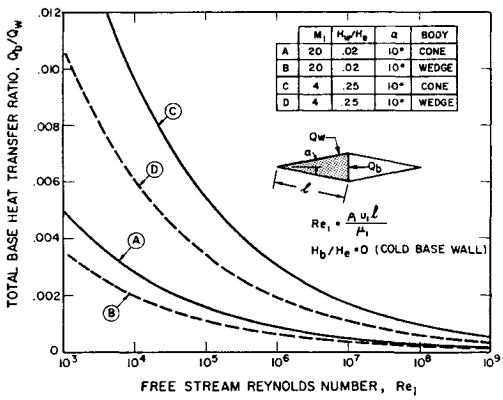

Fig. 10 Dependence of base heat transfer on flight Reynolds number.

for the undistorted initial profiles). For various flow conditions, the core enthalpy H_c can then be found in terms of the assumed base heat-transfer rate Q_b, as shown in Fig. 11. Note from this figure the sensitivity of H_c/H_e to the assumed ratio Q_b/Q_w. For example, for a 10° cone at $M_1 = 20$ and $H_w/H_e = 0.02$, if the actual total base heating rate is only about 4% of the body heating rate, the core would be cooled down to $H_c \approx 0$. Physically this cannot occur, since $Q_b \propto (H_c - H_b)$, and, in fact, the actual matched results of Fig. 10 for $H_b = 0$ are such that H_c is only slightly changed from the value corresponding to an adiabatic base. Experimental base heat-transfer rates could conceivably be higher than those of Fig. 10, however, and the steep slopes of the curves of Fig. 11 would then imply that base heat transfer has a more important effect on the base flow than that predicted by the present analysis.

Results with Mass Injection

Mass injection may be applied either on the upstream body surface or from the base wall (or in both places). As one might expect from experience with attached boundary layers, large effects may be obtained with relatively small expenditures of injection gas. Since we do not have space to discuss this subject at great length, we shall attempt only to describe the physical effects on the base flow due to mass injection.

When blowing occurs on the upstream body surface (as from ablation) the primary effects on the base flow are due

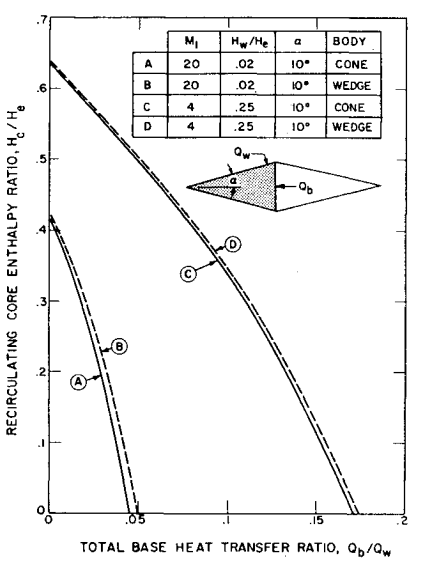

Fig. 11 Effect of base heat transfer on the recirculating core enthalpy.

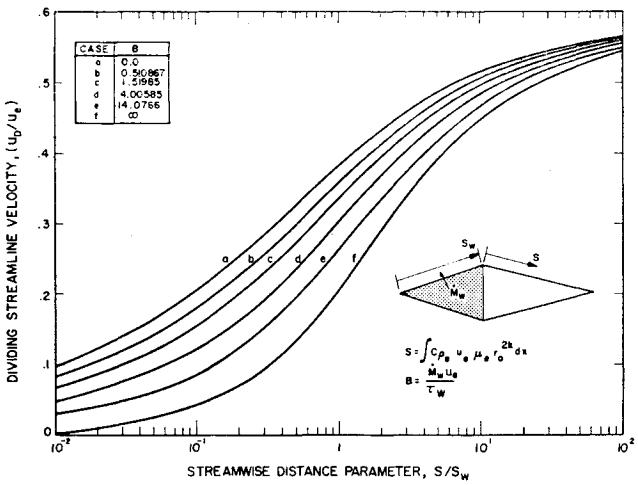

Fig. 12 Dividing streamline velocity buildup with similar body blowing.

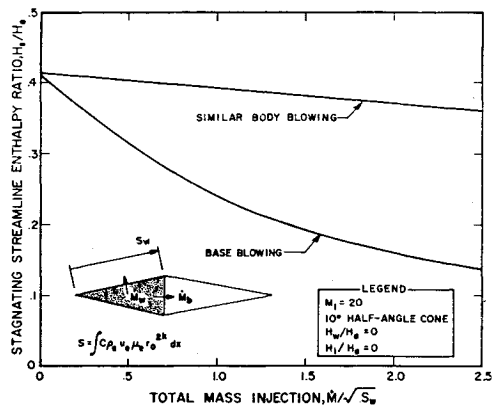

Fig. 14 Effect of blowing on the neck centerline enthalpy.

to the distortion of the initial profiles. Calculations have been carried out using the velocity profiles of Emmons and Leigh[15] for similar blowing, with the Crocco integral relation applying for the enthalpy. With increasing body blowing rates, the dividing streamline velocity grows more slowly (Fig. 12), and this causes a lengthening of the wake according to the Chapman recompression condition. The introduction of gas at the cold body wall temperature generally causes the over-all temperature levels in the base flow to be reduced, even though the longer wake causes more external high total enthalpy gas to be entrained in the energy control volume.

With base mass injection, it is assumed that the flow enters with negligible momentum (as through a porous plug). The shear-layer profiles are then unaffected, but the mass balance described earlier requires that the recompression condition be applied to a stagnating streamline with lower velocity than the dividing streamline. Figure 13, showing the velocity along various streamlines, illustrates this effect and implies that increasing the base bleed rate will also produce a longer wake. In fact, by blowing hard enough (still retaining the assumption of negligible injection gas momentum), it is possible to make the wake long enough for Chapman's similar solution to be applicable just before a negligibly strong recompression. In this case, the Crocco integral for the total enthalpy is approached and the maximum static enthalpy with injection of a cold gas similar to air approaches 0.25 H_e for large Mach numbers.

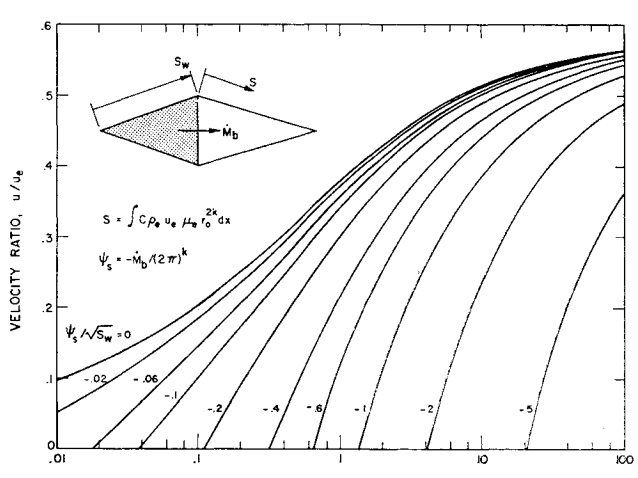

Fig. 13 Velocity along the stagnating streamline with base blowing.

The introduction of cold bleed gas directly into the recirculating core is very effective for cooling, and completely overshadows the heating effect due to the entrainment of additional freestream gas in the longer shear layer. Figure 14 gives a comparison of the stagnating streamline enthalpies for either body blowing or base blowing. It can be seen that, for the conditions noted, the base blowing appears more effective.

Figure 15 illustrates the effect of body or base blowing on the static enthalpy profiles after recompression. With no blowing, the maximum static enthalpy is on the centerline; however, as the blowing rate increases, the maximum static enthalpy may shift to an intermediate point in the profile. These considerations should be taken into account for downstream wake calculations.

The limiting profiles for high blowing rates are shown in Fig. 15 and illustrate the maximum cooling effect attainable with mass injection of similar gases.

Discussions and Conclusions

The preceding sections illustrate how the original Chapman separated flow model may be extended and employed to analyze the properties of the laminar base-flow region. Typical results are presented which suggest the following conclusions:

1) The shapes of the initial separated shear-layer profiles are extremely important in determining the structure of the laminar base flow.

2) For typical initial profiles, the separated layer is far too short for Chapman's similar solution to be valid, even near the recompression end. For cold wall conditions, the Crocco integral relation is never even approximately satisfied in the separated layer.

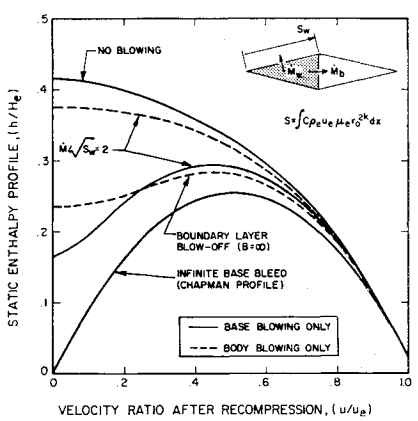

Fig. 15 Effect of blowing on the static enthalpy profile after recompression.

3) If the base heat-transfer rate is physically as small as that predicted by the present theory, the base heat transfer plays a relatively minor role in determining the properties of the base flow.

4) Mass transfer, either from the body surface or from the base, can be used to reduce the peak static enthalpy levels in the base-flow region. Base injection appears to be somewhat more effective for cooling than the same mass flow rate injected from the body surface.

Possible improvements to the base-flow theory within the present framework might be in the area of improved gas property relations for the shear-layer calculations and an improved inviscid-flow theory. However, it now appears that the Chapman model has been carried about as far as possible. The worth of the theory in its present form will have to be decided when definitive base-flow data become available. This applies especially to the application of the theory to high Mach number and low Reynolds number conditions. For example, ballistic range photos (such as Fig. 1) suggest that the neck region is sufficiently long so that the "step isentropic recompression" of the Chapman theory may be a poor assumption. The applicability of the Mangler transformation near the neck region of axisymmetric flows is certainly questionable, and it is quite possible that low Reynolds number effects (e.g., displacement thickness interaction) must be included when the analysis is applied to reentry conditions. Therefore, although considerable progress has been made with extensions of the Chapman model, consideration of the detailed process of recompression and recirculation may be necessary to adequately describe the laminar base flow.

References

[1] Chapman, D. R., "Laminar mixing of a compressible fluid," NACA TN 1800 (1950).

[2] Chapman, D. R., "An analysis of base pressure at supersonic velocities and comparison with experiment," NACA TN 2137 (1951).

[3] Chapman, D. R., "A theoretical analysis of heat transfer in regions of separated flow," NACA TN 3792 (1956).

[4] Chapman, D. R., Kuehn, D. M., and Larson, H. K., "Investigation of separated flows in supersonic and subsonic streams with emphasis on the effect of transition," NACA TN 3869 (1957).

[5] Denison, M. R. and Baum, E., "Compressible free shear layer with finite initial thickness," AIAA J. 1, 342–349 (1963).

[6] King, H. H. and Baum, E., "Enthalpy and atom profiles in the laminar separated shear layer," Electro-Optical Systems, Inc., Res. Note RN-8 (March 1963).

[7] Baum, E., "Effect of boundary layer blowing on the laminar separated shear layer," Electro-Optical Systems, Res. Note RN-9 (April 1963).

[8] King, H. H. and Baum, E., "Effect of base bleed on the laminar base flow," Electro-Optical Systems, Res. Note RN-10 (May 1963).

[9] King, H. H., "An analysis of base heat transfer in laminar flow," Electro-Optical Systems, Res. Note RN-14 (September 1963).

[10] Baum, E., "Effect of boundary layer distortion at separation on the laminar base flow," Electro-Optical Systems, Res. Note RN-16 (October 1963).

[11] King, H. H., "A tabulation of base flow properties for cones and wedges," Electro-Optical Systems, Res. Note RN-17 (December 1963).

[12] Goldstein, S., "Concerning some solutions of the boundary layer equations in hydrodynamics," Proc. Cambridge Phil. Soc. 26, 18–30 (1930).

[13] Baum, E., "Initial development of the laminar separated shear layer," AIAA J. 2, 128–131 (1964).

[14] Cohen, C. B. and Reshotko, E., "Similar solutions for the compressible laminar boundary layer with heat transfer and pressure gradient," NACA TN 3325 (1955).

[15] Emmons, H. W. and Leigh, D., "Tabulation of the Blasius function with blowing and suction," Combustion Aerodynamics Lab., Interim Tech. Rept. 9, Harvard Univ., Div. of Applied Science (1953).